Organic electroluminescent derivatives containing dibenzothiophene and diarylamine segments

Tai-Hsiang Huang,[a] Wha-Tzong Whang,*[a] Jiun Yi Shen,[b] Jiann T. Lin*[b] and Hegen Zheng[c]

A new series of 2,8-disubstituted dibenzothiophenes have been successfully synthesized *via* palladium-catalyzed C–N or C–C bond formation using 2,8-dibromodibenzothiophene and diarylamines as starting materials. These new dibenzothiophene derivatives are amorphous with a glass transition temperature ranging from 86 to 190 °C. Furthermore, they are fluorescent in the blue to bluish green region. Two types of light-emitting diodes (LED) were constructed from these compounds, (I) ITO/**Cpd**/TPBI/LiF/Al and (II) ITO/**Cpd**/Alq$_3$/LiF/Al, where TPBI and Alq$_3$ are 1,3,5-tris(*N*-phenylbenzimidazol-2-yl)benzene and tris(8-hydroxyquinolinato)aluminium, respectively. In type I devices, the compounds function as the hole-transporting and emitting material. In type II devices, emission from Alq$_3$ is observed. Several type I devices emit pure blue light, and most of the devices II have very promising performance. The relation between the energy levels of the materials and the performance of the light-emitting diodes is discussed.

Introduction

The application of organic electroluminescent (OEL) in flat-panel displays using small organic molecules[1] or organic polymers[2] has been intensively pursued after the works by Tang *et al.*[3] in 1987 and Friend *et al.* in 1990.[4] Presently the organic light emitting diodes (OLEDs) are considered to be the emissive display technology most competitive with the liquid crystal displays (LCDs). For full color display applications, efficient blue, green and red emitters with excellent color purity are very important. The amorphous character of the materials is also important in multilayer devices in order to reduce the formation of grain boundaries during the long-term operation.[5] Therefore, Shirota and co-workers have synthesized several novel families of organic π-electron star-shaped molecules which readily form amorphous glasses above room temperature.[1a] Thompson's group also examined a series of triarylamino moieties which were indeed beneficial to glass formation.[6] Our strategy to construct amorphous materials for OLED applications is to encapsulate the emitting π-conjugated luminophore cores with peripheral diarylamines. In our previous reports, we have developed high performance carbazole derivatives,[7] amorphous 2,3-disubstituted thiophenes,[8] efficient blue-emitting anthracenes,[9] and excellent thermally stable spirobifluorene derivatives.[10]

In this study, we introduce diarylamine moieties at the 2- and 8-positions of a dibenzothiophene core in order to obtain amorphous materials. Excessive conjugation *via* the 2,8-disubstituted dibenzothiophene core is not likely to occur,

and blue-emitting characteristic is expected for these materials. Here, we have successfully synthesized a series of dibenzothiophene derivatives containing peripheral diarylamines. Physical properties of these new compounds will be discussed. Two types of OEL devices were also fabricated for each of the compounds.

Results and discussion

Synthesis and optical properties

The 2,8-disubstituted dibenzothiophene derivatives (Chart 1) were conveniently prepared by two different palladium catalyzed cross coupling reactions (Scheme 1). (i) The catalyst developed by Koie *et al.*[11] and Hartwig *et al.*,[12] Pd(OAc)$_2$/P(t-Bu)$_3$ in the presence of *t*-BuONa, efficiently catalyzed aromatic C–N bond formation from 2,8-dibromodibenzothiophene[13] and secondary arylamines to provide the tertiary arylamines **S-1**–**S-6**. (ii) Appropriate triarylamines were converted to their boronic acids, which were then subjected to Suzuki reaction[14] with 2,8-dibromodibenzothiophene to form the desired compounds (major: **S-3** and minor: **S-4**). The absorption and luminescence data of the compounds are presented in Table 1. Representative absorption and emission spectra are shown in Fig. 1 and Fig. 2. In general, they display absorption resulting from the combination of dibenzothiophene and benzene, naphthalene, or pyrene chromophores and cover the entire UV-visible region (250–450 nm). The monosubstituted compound **S-4** has a similar electronic profile to the disubstituted one (**S-3**), indicating that there was no significant electronic coupling between the two arylamine segments. In accordance with this, **S-4** also has smaller absorption extinction coefficient than **S-3**. No discrete charge transfer bands are found in these compounds and the pyrene-containing compounds display a distinct absorption at the longer wavelength due to the localized pyrene π → π* transition. These diamines are weakly to moderately photoluminescent with emission wavelengths

[a]Department of Materials Science and Engineering, National Chiao Tung University, 1001 Ta Hsueh Rd, Hsin Chu 300, Taiwan
[b]Institute of Chemistry, Academia Sinica, 128 Sec. 2, Academia Rd, Nankang, Taipei 115, Taiwan. E-mail: jtlin@chem.sinica.edu.tw; Fax: 886-2-27831237; Tel: 886-2-27898522
[c]Coordination Chemistry Institute and Department of Chemistry, Nanjing University, Nanjing, 210093, P.R. China
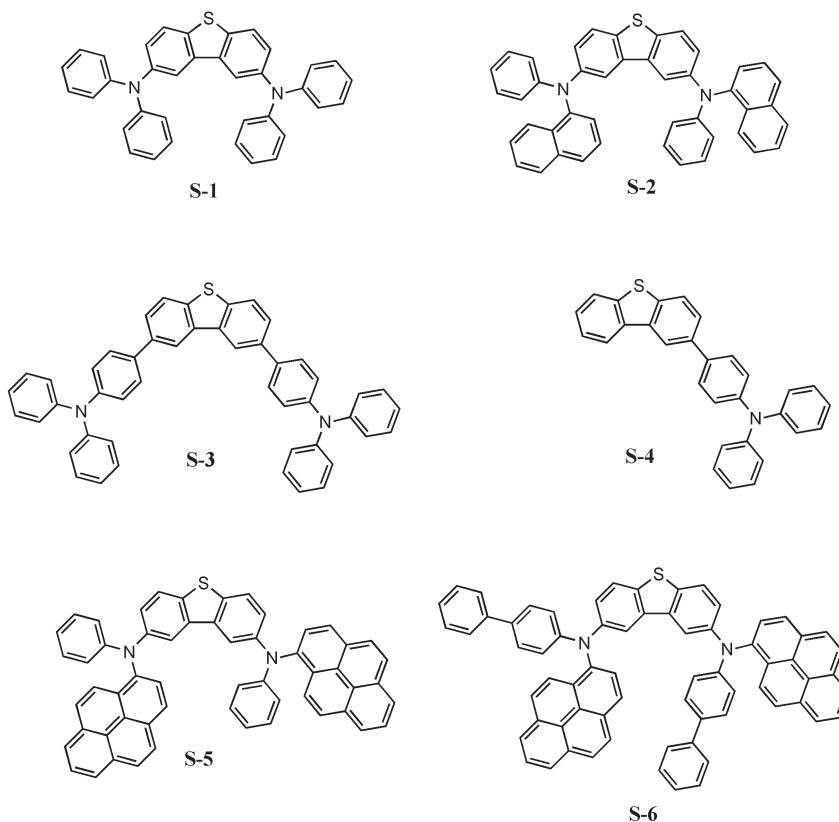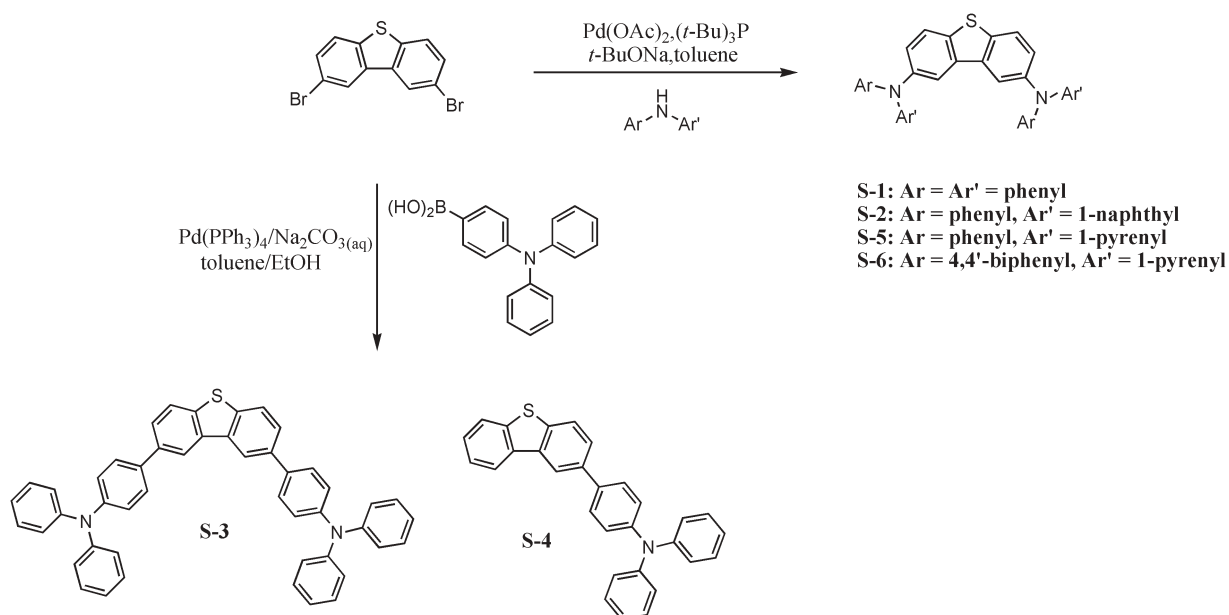
This journal is © The Royal Society of Chemistry 2005

J. Mater. Chem., 2005, **15**, 3233–3240 | 3233

Chart 1   Structures of the compounds.

S-1: Ar = Ar' = phenyl
S-2: Ar = phenyl, Ar' = 1-naphthyl
S-5: Ar = phenyl, Ar' = 1-pyrenyl
S-6: Ar = 4,4'-biphenyl, Ar' = 1-pyrenyl

**Scheme 1**   Synthesis of compounds **S-1–S-6**.

ranging from purple blue to blue green. Among the compounds with 2,8-diarylamine substituents, those containing a pyrene moiety (**S-5** and **S-6**) emit blue green light ($\lambda_{em} > 495$ nm) in CH_2Cl_2 solution, while a prominent blue shift in luminescent spectra is observed when both pyrene substituents are replaced by benzene (**S-1**; $\Delta\lambda = 65$ nm), naphthalene (**S-2**; $\Delta\lambda = 70$ nm) and triphenylamine (**S-3**; $\Delta\lambda = 75$ nm). Though it is common for pyrene derivatives to form excimers upon excitation,[15] there is no evidence of excimer formation in our compounds even up to a concentration of 1.0×10^{-3} M.

Table 1 Physical data of the compounds

Parameter		S-1	S-2	S-3	S-4	S-5	S-6
λ_{abs} (log ε)[a]	toluene	305(4.6), 358(3.8)	309(4.5), 351(4.1)	333(4.7)	331(4.4)	315(4.7), 388(4.3), 410(4.1)	331(4.8), 389(4.2), 414(4.2)
	CH_2Cl_2	266(4.5), 306(4.7), 356(3.9)	264(4.6), 307(4.5), 351(4.2)	253(4.6), 307(4.5), 335(4.7)	247(4.6), 332(4.4)	264(4.7), 315(4.6), 384(4.3), 404(4.2)	245(4.8), 331(4.3), 384(4.3), 410(4.3)
λ_{em} (Φ_f [%])[b]	toluene	422(4)	429(7)	406(58)	402(65)	470(73)	473(70)
	CH_2Cl_2	435(4)	454(11)	425(58)	420(71)	498(78)	501(79)
	film	437	445	430	431	494	501
T_m, T_c, (T_g/T_d)[c]/°C		206, NA, 86/321	NA, NA, 112/384	210, NA, 93/475	197, NA, 88/350	248, NA, 165/485	248, NA, 190/505
E (ΔE_p)[c]/mV		446(100), 634(120)	459(84), 670(126)	467(125)	484(101)	386(95), 519(99)	370(85), 496(87)
HOMO[d]/eV		4.98	4.98	4.98	5.01	4.91	4.89
LUMO[d]/eV		1.93	1.94	1.86	1.83	2.19	2.20
Band gap[d]/eV		3.05	3.04	3.12	3.18	2.72	2.69

[a] Measured in a concentration of 5.0×10^{-5} M. [b] Quantum yield was measured relative to coumarin 6 (63% in CH_3CN). Corrections due to the change in solvent refractive indices were applied. Excitation wavelength was 350 nm for all compounds. [c] Measured in CH_2Cl_2. All the potentials are reported relative to ferrocene, which was used as the internal standard in each experiment. Ferrocene oxidation potential was located at +332 mV relative to the Ag/AgNO₃ nonaqueous reference electrode. The concentration of the compound was 1.0×10^{-3} M. [d] HOMO energy was calculated with reference to ferrocene (4.80 eV). Solvent to vacuum correction was not applied. Band gap was derived from the observed optical edge and LUMO energy was derived from the relation, band gap = HOMO − LUMO.
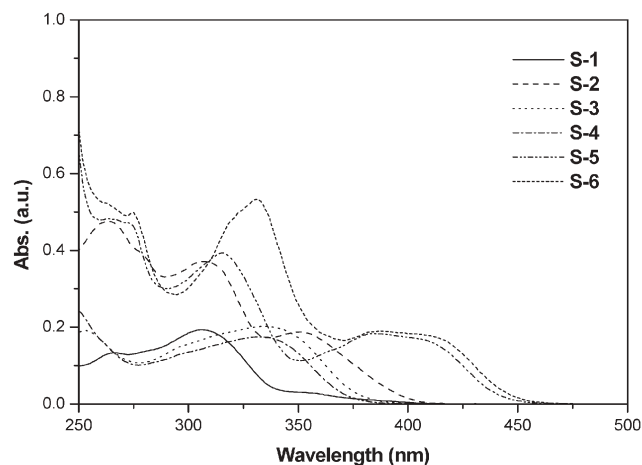
Fig. 1 The absorption spectra of the compounds (5.0×10^{-5} mol L^{-1} in dichloromethane).
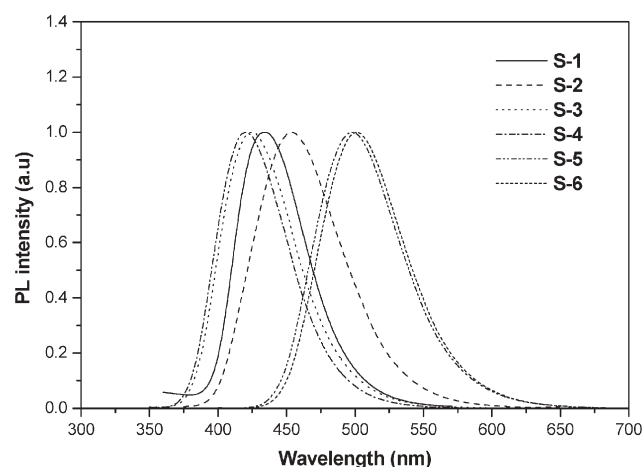
Fig. 2 The emission spectra of the compounds (5.0×10^{-6} mol L^{-1} in dichloromethane). The excitation wavelength is 350 nm.
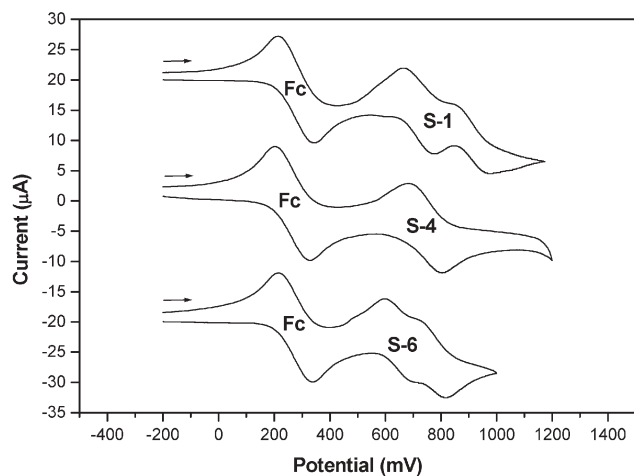
Thermal properties

The glass forming capability and thermal stability of these materials were determined by DSC (differential scanning calorimetry) and TGA (thermogravimetric analysis) measurements. The detailed data are collected in Table 1. Compounds **S-3** to **S-6** exhibited sequential glass transition, melting, but no crystallization behavior upon repetitive heating and cooling cycles in DSC plots. Compound **S-2** exhibited a glass transition after the first heating cycle, and no crystallization exotherm and melting endotherm were noticed. Compound **S-1** exhibited melting isotherms during the first heating cycle, but rapid cooling of the melt led to the formation of a glassy state which persisted in the subsequent heating cycles. The disubstituted dibenzothiophene derivative (**S-3**) displayed a higher T_g when compared to its monosubstituted analogue (**S-4**). Similarly, incorporation of pyrene in the structure leads to a significant enhancement in the T_g. For instance, in the series **S-5** and **S-6** the role of pyrene is clearly evident (**S-5**: T_g = 165 °C and **S-6**: T_g = 190 °C). Both **S-5** and **S-6** possess remarkably high T_g values, they also have the highest

This journal is © The Royal Society of Chemistry 2005

J. Mater. Chem., 2005, **15**, 3233–3240 | 3235

decomposition temperatures (>480 °C) among all the compounds studied. In addition, compare **S-1** (T_g = 86 °C) with commonly used hole-transport materials, such as 1,4-bis(diphenylamino)biphenyl (DDB, T_g = 77 °C) and **S-2** (T_g = 112 °C) with 1,4-bis(1-naphthylphenylamino)biphenyl (α-NPD, T_g = 100 °C).[16] Although the peripheral diarylamines of the selective compounds are almost the same, there is a slight increase in T_g after replaced the biphenyl ring by a dibenzothiophene segment.
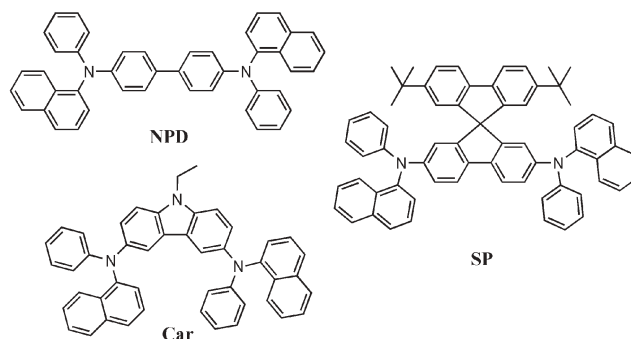
Electrochemical properties

Electrochemical characteristics of the dibenzothiophene derivatives were studied by using cyclic and differential pulse voltammetric methods. The first oxidation potentials were used to determine the HOMO (highest occupied molecular orbital) energy levels. Ferrocene served as an internal standard for calibrating the potential and calculating the HOMO levels (−4.8 eV).[17a,b] The redox potentials of these materials are listed in Table 1.

In general, all the molecules undergo a reversible one- or two-electron oxidation at low positive potentials result from terminal diarylamino units at the 2- or 8-position of the dibenzothiophene core. The typical cyclic voltammetric behavior is shown in Fig. 3 for **S-1**, **S-4** and **S-6**. The two one-electron oxidation processes observed in the compounds **S-1**, **S-2**, **S-5**, and **S-6** indicate that the two amino groups are affected electronically by each other *via* the sulfur atom at the core. Insertion of an extra phenyl ring between the dibenzothiophene core and the peripheral diarylamine (**S-3** and **S-4**) diminishes such electronic communication, and the two amines are oxidized simultaneously. The oxidation potential increases in order of **S-6** < **S-5** < **S-1** ≈ **S-2** < **S-3** ≈ **S-4** and is consistent with the electron-donating ability of the substituents at the nitrogen atom. A comparison was made of the difference of the first and second oxidation potentials, E_{2-1}, between **S-2** with those also containing a biphenyl skeleton (Fig. 4). They are in order of **S-2** < **NPD** < **SP** < **Car**.[7,10,17c] In **SP** and **NPD**, the two peripheral amines have electronic communication *via* the biphenyl skeleton directly. The more
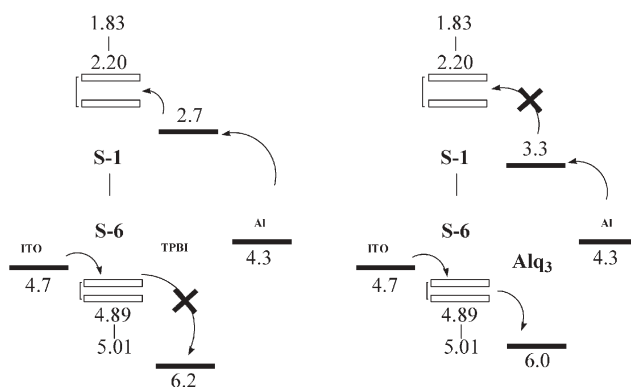

Fig. 4 Compounds containing a biphenyl skeleton.

planar conformation of the two phenyl rings in **SP** apparently allows more efficient conjugation. On the other hand, the two peripheral amines are expected to communicate with each other *via* the central sulfur and nitrogen atoms, respectively. The more electron-donating character of the central amine in **Car** couples the two peripheral amines efficiently, and E_{2-1} even surpasses those of **SP** and **NPD**.

Electroluminescent properties

The HOMO energy levels of the compounds were calculated from cyclic voltammetry (*vide supra*) and by comparison with ferrocene (−4.8 eV).[18] These data together with absorption spectra were then used to obtain the LUMO (lowest unoccupied molecular orbital) energy levels (Table 1, Scheme 2). The compounds in this study appear to be appropriate as hole-transporting and emitting materials.

These amorphous dibenzothiophene derivatives were subjected to fabrication of two types of double-layer devices using TPBI (1,3,5-tris(*N*-phenylbenzimidazol-2-yl)benzene) or Alq₃ (tris(8-hydroxyquinoline)aluminium) as the electron-transport materials: (I) ITO/**Cpd** (40 nm)/TPBI (40 nm)/LiF (1 nm)/Al (150 nm); (II) ITO/**Cpd** (40 nm)/Alq₃ (40 nm)/LiF (1 nm)/Al (150 nm) (where **Cpd** means the dibenzothiophene derivatives). The performance parameters of all devices are collected in Table 2. The current–voltage (*I*–*V*) and luminance–current (*I*–*L*) characteristics are shown in Figs. 5 and 6. Fig. 7 exhibits the electroluminescent (EL) spectra of devices I and II. Green light characteristic of Alq₃ was emitted from type II devices (λ_{max} ~ 522 nm), whereas type I devices emitted blue to

Fig. 3 Cyclic voltammogram of the compounds measured in dichloromethane solution.

Scheme 2 The relative energy alignments of the materials in devices.

Table 2 Electroluminescent data of the devices[a]

	S-1	S-2	S-3	S-4	S-5	S-6
V_{on}/V	3.0; 2.5	3.0; 2.5	3.0; 2.5	3.5; 3.0	3.0; 2.5	3.0; 2.5
$L_{max}/cd\ m^{-2}$ (V at L_{max}/V)	1973 (14.5); 36329 (15)	3855 (13); 53235 (15)	9832 (11.5); 50096 (15)	4271 (12.5); 36276 (15)	36301 (13); 56224 (15)	40222 (15); 38467 (15)
λ_{em}/nm	444; 522	442; 522	428; 520	428; 522	480; 520	498; 522
CIE $(x;y)$	0.17, 0.17; 0.30, 0.55	0.15, 0.08; 0.30, 0.55	0.16, 0.05; 0.30, 0.55	0.16, 0.07; 0.30, 0.55	0.17, 0.35; 0.29, 0.53	0.17, 0.50; 0.31, 0.55
fwhm/nm	96; 96	62; 94	56; 94	64; 96	74; 96	56; 96
$\eta_{ext,max}$ (%)	0.42; 1.44	0.99; 1.46	4.56; 1.67	1.92; 1.58	3.33; 2.00	2.80; 2.22
$\eta_{p,max}/lm\ W^{-1}$	0.55; 4.22	0.69; 4.33	1.53; 4.69	0.71; 3.80	7.55; 5.97	7.34; 7.10
$\eta_{c,max}/cd\ A^{-1}$	0.52; 4.59	0.66; 4.67	2.04; 5.28	1.03; 4.99	7.20; 6.09	7.29; 7.07
$L/cd\ m^{-2}$ *	373; 4557	525; 4668	1831; 5267	920; 4806	5386; 5984	6821; 6565
η_{ext} (%) *	0.31; 1.43	0.79; 1.46	4.13; 1.67	1.72; 1.54	2.50; 1.93	2.63; 2.07
$\eta_{p}/lm\ W^{-1}$ *	0.23; 2.38	0.30; 3.03	0.92; 2.71	0.44; 2.14	3.16; 3.37	4.25; 3.82
$\eta_{c}/cd\ A^{-1}$ *	0.38; 4.56	0.53; 4.67	1.84; 5.27	0.92; 4.84	5.41; 6.00	6.84; 6.58

[a] The measured values are given in the order of the devices I and II. L_{max}, maximum luminance; L, luminance; V, voltage; V_{on}, turn-on voltage; $\eta_{ext,max}$, maximum external quantum efficiency; $\eta_{p,max}$, maximum power efficiency; $\eta_{c,max}$, maximum current efficiency; η_{ext}, external quantum efficiency; η_{p}, power efficiency; η_{c}, current efficiency; fwhm, full width at half maximum. *, at a current density of 100 mA cm^{-2}. V_{on} was obtained from the x-intercept of a log(luminance) vs. applied voltage plot.
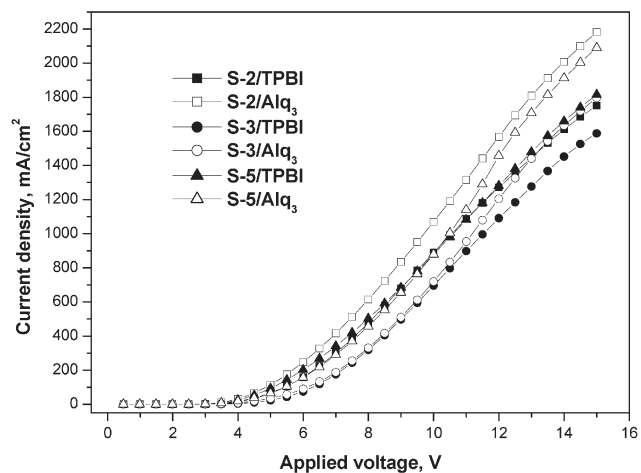

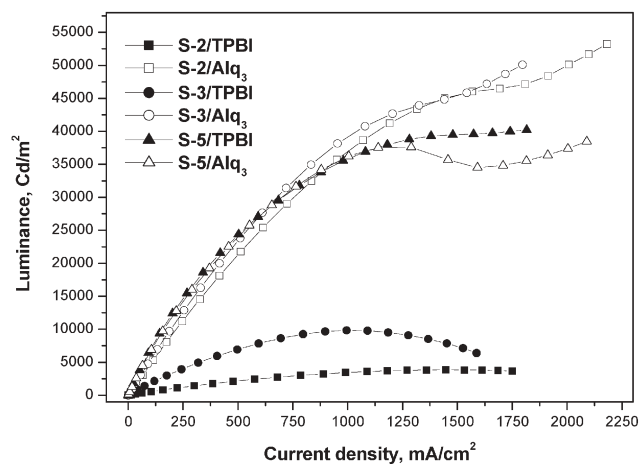**Fig. 5** Current density *vs.* applied electric voltage characteristics of selected compounds.

Fig. 6 Selected luminance *vs.* current density characteristics of the devices.
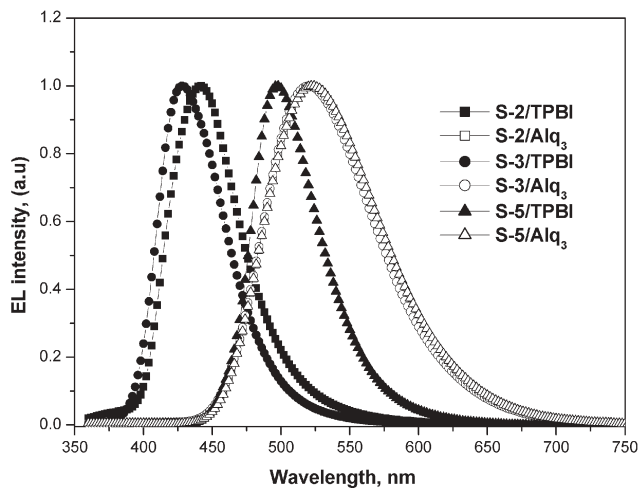

Fig. 7 The EL spectra of the selected devices.

greenish blue light from the **Cpd** compounds. The EL spectra of type I devices for all the compounds were nearly super-imposable with the film PL spectra. Such an outcome can be rationalized by the HOMO energy gaps between the hole-transport and electron-transport materials. The HOMO energy gap of Alq$_3$ (ΔE = 0.99–1.11 eV) is less than that between compounds and TPBI (ΔE = 1.31–1.19 eV), and passage of holes from **Cpd** into the Alq$_3$ layer in devices II is expected. In contrast, the passage of holes from the **Cpd** layer to the TPBI layer is effectively blocked due to the low-lying HOMO energy level of TPBI (HOMO = 6.2 eV).[19] On the other hand, all the dibenzothiophene derivatives effectively serve as the electron-blocking material in device II due to the large LUMO energy gap between **Cpd** and Alq$_3$ (ΔE = 1.10–1.47 eV). Passage of the electrons from ETL to HTL is more facile in device I because of the much smaller LUMO energy gap (ΔE = 0.50–0.83 eV) between **Cpd** and TPBI.

All the devices in this study show relatively low turn-on voltages (2.5–3.5 V) and operating voltages (5.1–7.2 V at a current density of 100 mA cm^{-2}). The devices I of **S-1–S-4** emit blue light. Among them, the Commission International de l'Éclairage (CIE) coordinates (x,y) of **S-2–S-4** are located in pure blue region: (0.15, 0.08), (0.16, 0.05), and (0.16, 0.07) for **S-2**, **S-3**, and **S-4**, respectively. While no optimization has been made on the type II devices, the performance parameters appear to be promising: maximum luminescence (36276–56224 cd m^{-2}), maximum external quantum efficiency (1.44–2.22%), and maximum luminous efficiency (3.80–7.10 lm W^{-1}). These values are in general better than those of typical green light-emitting devices based on the structure ITO/diamine/Alq$_3$/LiF/Al with similar device structure.[19e,f] A standard device of the structure ITO/α-NPD (40 nm)/Alq$_3$ (40 nm)/LiF(1 nm)/Al(150 nm) was also fabricated for comparison and found to have a maximum luminescence of 34078 cd m^{-2} at 15 V, a maximum external quantum efficiency of 1.04% at 5 V, and a maximum luminous efficiency of 3.10 lm W^{-1} at 3.0 V. It is interesting to note that the performance parameters for the device I of **S-3** are two times greater than those of **S-4**. For instance, at 100 cd cm^{-2} current density: luminescence, 1831 (**S-3**) *vs.* 920 cd m^{-2} (**S-4**); external quantum efficiency, 4.1 (**S-3**) *vs.* 1.7% (**S-4**); luminous efficiency, 0.92 (**S-3**) *vs.* 0.44 lm W^{-1} (**S-4**); current efficiency, 1.8 (**S-3**) *vs.* 0.92 cd A^{-1} (**S-4**). Such an outcome may be due to a better balance of the carriers, or a smaller contact resistance for the device of **S-3**.

Conclusions

In summary, we have synthesized a series of new luminophores with a 2,8-disubstituted dibenzothiophene core and peripheral diarylamines or triarylamine *via* palladium-catalyzed C–N bond formation and C–C bond Suzuki coupling reaction. These amorphous compounds emit blue to greenish blue. Double-layer devices which emit pure blue light can be fabricated using these compounds as the hole-transporting and emitting materials. Double-layer devices using the compounds as the hole-transporting materials, and Alq$_3$ as the electron-transporting and emitting materials exhibit very promising performance. Further extension to other n-type

electroluminscent materials constructed from a dibenzothiophene core is ongoing.

Experimental

Unless otherwise specified, all the reactions were carried out under nitrogen atmosphere using standard Schlenk techniques. Solvents were dried by standard procedures. All column chromatography was performed with the use of silica gel (230–400 mesh, Macherey-Nagel GmbH & Co.) as the stationary phase. The ^{1}H NMR spectra were recorded on a Bruker AC300 or AMX400 spectrometer. Electronic absorption spectra were measured in various solvents using a Cary 50 Probe UV-visible spectrophotometer. Emission spectra were recorded by a Hitachi F-4500 fluorescence spectrometer. Emission quantum yields were measured with reference to coumarin 1 or coumarin 6 in CH$_3$CN.[20] Cyclic voltammetry experiments were performed with a BAS-100 electrochemical analyzer. All measurements were carried out at room temperature with a conventional three-electrode configuration consisting of platinum working and auxiliary electrodes and a nonaqueous Ag/AgNO$_3$ reference electrode. The $E_{1/2}$ values were determined as $1/2(E_p^a + E_p^c)$, where E_p^a and E_p^c are the anodic and cathodic peak potentials, respectively. The solvent in all experiments was CH$_2$Cl$_2$ and the supporting electrolyte was 0.1 M tetrabutylammonium perchlorate. DSC measurements were carried out using a Perkin-Elmer 7 series thermal analyzer at a heating rate of 10 °C min^{-1}. TGA measurements were performed on a Perkin-Elmer TGA7 thermal analyzer. Mass spectra (FAB) were recorded on a JMS-700 double focusing mass spectrometer (JEOL, Tokyo, Japan). Elementary analyses were performed on a Perkin-Elmer 2400 CHN analyzer.

Compound N,N,N',N'-tetraphenyl-dibenzothiophene-2,8-diamine (**S-1**), N,N'-di-naphthalen-1-yl-N,N'-diphenyl-dibenzothiophene-2,8-diamine (**S-2**), N,N'-diphenyl-N,N'-di-pyren-1-yl-dibenzothiophene-2,8-diamine (**S-5**) and N,N'-bis-biphenyl-4-yl-N,N'-di-pyren-1-yl-dibenzothiophene-2,8-diamine (**S-6**) were synthesized by a procedure similar to the following description. A two-necked round-bottomed flask was charged with Pd(OAc)$_2$ (1 mmol% per halogen atom), t-BuONa (1.2 equiv. per halogen atom), halides (5 mmol), and amines (2 equiv. per halogen atom). Dry toluene was added, and the reaction was stirred under nitrogen for 10 min. Tri-*tert*-butylphosphine (2 mmol%) in dry toluene was added through a syringe (the stock solution contained 1.0 mmol of the phosphine in 1 mL of dry toluene). The reaction mixture was heated at 90 °C for 20 h. After cooling, the mixture was diluted with ether and the organic phase was washed with water and brine. After drying over MgSO$_4$ and removing of the volatiles, the residue was purified by column chromatography using CH$_2$Cl$_2$–n-hexane as eluent and followed by recrystallization from CH$_2$Cl$_2$ and MeOH.

Compound (S-1), white solid, yield = 68% (860 mg). ^{1}H NMR (CDCl$_3$): δ 6.93–6.96 (m, 4 H, *para*-C$_6H_5$), 7.04–7.06 (m, 8 H, *ortho*-C$_6H_5$), 7.17–7.23 (m, 10 H, *meta*-C$_6H_5$, C$_6H_3$), 7.69 (d, 2 H, J = 8.6 Hz, C$_6H_3$), 7.72 (d, 2 H, J = 2.0 Hz, C$_6H_3$). FAB MS (m/z): 518 (M$^+$) Anal. Calcd for C$_{36}H_{26}N_2$S: C, 83.36; H, 5.05; N, 5.40. Found: C, 83.34; H, 5.02; N, 5.36%.

Compound (S-2), white solid, yield = 72% (960 mg). ^{1}H NMR (CDCl$_3$): δ 6.87 (t, 2 H, J = 7.4 Hz, *para*-C$_6$H$_5$), 6.91 (d, 4 H, J = 7.7 Hz, *ortho*-C$_6$H$_5$), 7.10–7.15 (m, 6 H, C$_6$H$_3$, *meta*-C$_6$H$_5$), 7.26–7.32 (m, 4 H, C$_{10}$H$_7$), 7.39–7.45 (m, 4 H, C$_{10}$H$_7$), 7.59 (d, 2 H, J = 8.6 Hz, C$_6$H$_3$), 7.71–7.74 (m, 4 H, C$_6$H$_3$, C$_{10}$H$_7$), 7.85 (d, 2 H, J = 6.7 Hz, C$_{10}$H$_7$), 7.93 (d, 2 H, J = 8.4 Hz, C$_{10}$H$_7$). FAB MS (*m/z*): 618 (M$^+$) Anal. Calcd for C$_{44}$H$_{30}$N$_2$S: C, 85.40; H, 4.89; N, 4.53. Found: C, 85.88; H, 4.95; N, 4.32%.

Compound (S-5), yellow solid, yield = 80% (1.12 g). ^{1}H NMR (CDCl$_3$): δ 6.85 (t, 2 H, J = 7.3 Hz, *para*-C$_6$H$_5$), 6.91 (d, 4 H, J = 7.6 Hz, *ortho*-C$_6$H$_5$), 7.10 (t, 4 H, J = 7.3 Hz, *meta*-C$_6$H$_5$), 7.22 (dd, 2 H, J_1 = 2.0 Hz, J_2 = 8.7 Hz, C$_6$H$_3$), 7.76–7.81 (m, 4 H, pyrenyl), 7.85 (d, 2 H, J = 2.0 Hz, C$_6$H$_3$), 7.92 (d, 2 H, J = 9.3 Hz, pyrenyl), 8.01 (t, 2 H, J = 7.6 Hz, pyrenyl), 8.07–8.19 (m, 10 H, C$_6$H$_3$, pyrenyl), 8.24 (d, 2 H, J = 7.6 Hz, pyrenyl). FAB MS (*m/z*): 766 (M$^+$) Anal. Calcd for C$_{56}$H$_{34}$N$_2$S: C, 87.70; H, 4.47; N, 3.65. Found: C, 87.98; H, 4.41; N, 3.58%.

Compound (S-6), yellow solid, yield = 69% (1.02 g). ^{1}H NMR (CDCl$_3$): δ 6.98 (d, 4 H, J = 8.8 Hz, C$_6$H$_4$), 7.27 (t, 2 H, J = 7.4 Hz, *para*-C$_6$H$_5$), 7.30 (dd, 2 H, J_1 = 2.2 Hz, J_2 = 8.7 Hz, C$_6$H$_3$), 7.38 (t, 4 H, J = 7.3 Hz, *meta*-C$_6$H$_5$), 7.45 (d, 4 H, J = 8.8 Hz, C$_6$H$_4$), 7.52–7.55 (m, 4 H, *ortho*-C$_6$H$_5$), 7.83–7.86 (m, 4 H, C$_6$H$_3$, pyrenyl), 7.95 (d, 2 H, J = 9.3 Hz, pyrenyl), 7.99–8.04 (m, 6 H, pyrenyl), 8.10 (d, 2 H, J = 1.7 Hz, C$_6$H$_3$), 8.15 (d, 4 H, J = 9.2 Hz, pyrenyl), 8.21 (d, 2 H, J = 8.2 Hz, pyrenyl), 8.24 (d, 2 H, J = 7.6 Hz, pyrenyl). FAB MS (*m/z*): 918 (M$^+$) Anal. Calcd for C$_{68}$H$_{42}$N$_2$S: C, 88.86; H, 4.61; N, 3.05. Found: C, 88.40; H, 4.73; N, 2.97%.

Compounds *N,N*-diphenyl-4-8-[4-(diphenylamino)phenyl]-dibenzo[*b,d*]thiophen-2-ylaniline (**S-3**) and (4-dibenzothiophen-2-yl-phenyl)-diphenyl-amine (**S-4**) were synthesized by a similar procedure as described below. To a flask containing the 4-(diphenylamino)phenylboronic acid (2.5 equiv. per halogen atom), 2,8-dibromo-dibenzothiophene (0.20 mmol), and Pd(PPh$_3$)$_4$ (2 mmol% per halogen atom) was added 50 mL of toluene, 10 mL EtOH and 5 equiv. 2 M Na$_2$CO$_{3(aq)}$. The solution was stirred under reflux for 2 days. After cooling, the product was extracted with ether and the organic phase was washed with water and brine. Organic layer was dried over anhydrous MgSO$_4$ and removing of the volatiles. The residue was purified by column chromatography using CH$_2$Cl$_2$–n-hexane as eluent and followed by recrystallization from CH$_2$Cl$_2$ and MeOH. Compound **S-3** is the major and compound **S-4** is the minor product of this reaction.

Compound (S-3), pale yellow solid, yield = 42% (965 mg). ^{1}H NMR (CDCl$_3$): δ 7.03 (t, 4 H, J = 7.4 Hz, *para*-C$_6$H$_5$), 7.13–7.19 (m, 12 H, C$_6$H$_4$, *ortho*-C$_6$H$_5$), 7.25–7.29 (m, 8 H, J = 7.8 Hz, *meta*-C$_6$H$_5$), 7.57 (d, 4 H, J = 8.6 Hz, C$_6$H$_4$), 7.67 (dd, 2 H, J_1 = 1.5 Hz, J_2 = 7.9 Hz, C$_6$H$_3$), 7.87 (d, 2 H, J = 8.3 Hz, C$_6$H$_3$), 8.35 (d, 2 H, J = 1.5 Hz, C$_6$H$_3$). FAB MS (*m/z*): 670 (M$^+$) Anal. Calcd for C$_{48}$H$_{34}$N$_2$S: C, 85.94; H, 5.11; N, 4.18. Found: C, 85.87; H, 4.69; N, 4.03%.

Compound (S-4), pale yellow solid, yield = 25% (360 mg). ^{1}H NMR (CDCl$_3$): δ 7.03 (t, 2 H, J = 7.3 Hz, *para*-C$_6$H$_5$), 7.13–7.19 (m, 6 H, C$_6$H$_4$, *ortho*-C$_6$H$_5$), 7.27 (t, 4 H, J = 7.4 Hz, *meta*-C$_6$H$_5$), 7.44–7.48 (m, 2 H, C$_6$H$_4$ of dibenzothiophene), 7.57 (d, 2 H, J = 6.8 Hz, C$_6$H$_4$), 7.66 (dd, 1 H, J_1 = 1.8 Hz,

J_2 = 8.3 Hz, C$_6$H$_3$), 7.84–7.88 (m, 2 H, C$_6$H$_3$, C$_6$H$_4$ of dibenzothiophene), 8.18–8.21 (m, 1 H, C$_6$H$_4$ of dibenzothiophene), 8.31 (d, 1 H, J = 1.8 Hz, C$_6$H$_3$). FAB MS (*m/z*): 427 (M$^+$) Anal. Calcd for C$_{30}$H$_{21}$NS: C, 84.27; H, 4.95; N, 3.28. Found: C, 84.02; H, 4.86; N, 3.13%.

LEDs fabrication and measurement

Electron-transporting materials TPBI (1,3,5-tris(*N*-phenyl-benzimidazol-2-yl)benzene)[21] and Alq$_3$ (tris(8-hydroxyquino-line)aluminium)[22] were prepared by literature procedures, and were sublimed twice prior to use. Prepatterned ITO substrates with an effective individual device area of 3.14 mm^2 were cleaned as described in a previous report.[22] The thermal evaporation of organic materials was carried out following the previous procedures.[23] Double-layer EL devices using compounds **S-1–S-6** as the hole-transporting/emitting layer and TPBI or Alq$_3$ as the electron-transporting layer were fabricated. The devices were prepared by vacuum deposition of 40 nm of the hole-transporting layer, followed by 40 nm of TPBI or Alq$_3$. Inorganic LiF was evaporated to be the 1 nm buffer layer. Alumina rods were deposited as the cathode, which was capped with 100 nm of excess alumina. *I*–*V* curves were measured in a Keithley 2400 Source Meter in ambient environment. Light intensity was measured with a Newport 1835 Optical Meter.

References

1 (*a*) Y. Shirota, *J. Mater. Chem.*, 2000, **10**, 1; (*b*) P. Lu, H. Hong, G. Cai, P. Djurovich, W. P. Weber and M. E. Thompson, *J. Am. Chem. Soc.*, 2000, **122**, 7480; (*c*) Y. Shirota, M. Kinoshita, T. Noda, K. Okumoto and T. Ohara, *J. Am. Chem. Soc.*, 2000, **122**, 11021; (*d*) A. W. Freeman, S. C. Koene, P. R. L. Malenfant, M. E. Thompson and J. M. J. Fréchet, *J. Am. Chem. Soc.*, 2000, **122**, 12385; (*e*) C. Wang, G.-Y. Jung, Y. Hua, C. Pearson, M. R. Bryce, M. C. Petty, A. S. Batsanov, A. E. Goeta and J. A. K. Howard, *Chem. Mater.*, 2001, **13**, 1167; (*f*) Y.-T. Tao, E. Balasubramian, A. Danel, B. Jarosz and P. Tomasik, *Chem. Mater.*, 2001, **13**, 1207.

2 (*a*) U. Mitschke and P. Bäuerle, *J. Mater. Chem.*, 2000, **10**, 1471; (*b*) T. Miteva, A. Meisel, W. Knoll, H. G. Nothofer, U. Scherf, D. C. Müller, K. Meerholz, A. Yasuda and D. Neher, *Adv. Mater.*, 2001, **13**, 565; (*c*) C. Wang, M. Kilitziraki, L.-O. Pålsson, M. R. Bryce, A. P. Monkman and I. D. W. Samuel, *Adv. Funct. Mater.*, 2001, **11**, 47; (*d*) J. Pei, W.-L. Yu, W. Huang and A. J. Heeger, *Macromolecules*, 2000, **13**, 2462; (*e*) S. Liu, X. Jiang, H. Ma, M. S. Liu and A. K.-Y. Jen, *Macromolecules*, 2000, **33**, 3514; (*f*) W. J. Ni, J. H. Su, K. Chen and H. Tian, *Chem. Lett.*, 1997, **26**, 101; (*g*) W. H. Zhu, C. Hu, K. C. Chen and H. Tian, *Synth. Met.*, 1998, **96**, 151.

3 C. W. Tang and S. A. VanSlyke, *Appl. Phys. Lett.*, 1987, **51**, 913.

4 J. H. Burroughes, D. D. C. Bradley, A. R. Brown, R. N. Marks, K. Mackay, R. H. Friend, P. L. Burns and A. B. Holms, *Nature*, 1990, **347**, 539.

5 P. Fenter, F. Schreiber, V. Bulovic and S. R. Forrest, *Chem. Phys. Lett.*, 1997, **277**, 521.

6 B. E. Koene, D. E. Loy and M. E. Thompson, *Chem. Mater.*, 1998, **10**, 2235.

7 K. R. Justin Thomas, J. T. Lin, Y.-T. Tao and C.-W. Ko, *Chem. Mater.*, 2001, **123**, 9404.

This journal is © The Royal Society of Chemistry 2005

J. Mater. Chem., 2005, **15**, 3233–3240 | 3239

8 Y.-Z. Su, J. T. Lin, Y.-T. Tao, C.-W. Ko, S.-C. Lin and S.-S. Sun, *Chem. Mater.*, 2002, **14**, 1884.

9 K. Danel, T.-H. Huang, J. T. Lin, Y.-T. Tao and C.-H. Chuen, *Chem. Mater.*, 2002, **14**, 3860.

10 J. Y. Shen, C. Y. Lee, T.-H. Huang, J. T. Lin, Y.-T. Tao and C.-H. Chien, *J. Mater. Chem.*, 2005, **15**, DOI: 10.1039/b501819f.

11 M. Nishiyama, T. Yamamoto and Y. Koie, *Tetrahedron Lett.*, 1998, **39**, 617.

12 J. F. Hartwig, M. Kawatsura, S. I. Hauck, L. M. Shaughnessy and J. Alcazar-Roman, *J. Org. Chem.*, 1999, **64**, 5575.

13 (*a*) J. J. Eisch, L. E. Hallenbeck and K. I. Han, *J. Am. Chem. Soc.*, 1986, **108**, 7763; (*b*) C. R. Neumoyer and E. D. Amstutz, *J. Am. Chem. Soc.*, 1947, **69**, 1920.

14 N. Miyaura and A. Suzuki, *Chem. Rev.*, 1995, **95**, 2457.

15 (*a*) T. Jin, K. Ichikawa and T. Koyama, *J. Chem. Soc., Chem. Commun.*, 1992, 499; (*b*) J.-H. Liao, C.-T. Chen and J.-M. Fang, *Org. Lett*, 2002, **4**, 561.

16 D. F. O'Brien, P. E. Burrows, S. R. Forrest, B. E. Koene, D. E. Loy and M. E. Thompson, *Adv. Mater.*, 1998, **10**, 1108.

17 (*a*) M. Thelakkat and H. Schmidt, *Adv. Mater.*, 1998, **10**, 219; (*b*) C. Hohle, U. Hofmann, S. Schloter, M. Thelakkat, P. Strohriegl, D. Haarer and S. Zilker, *J. Mater. Chem.*, 1999, **9**, 2205; (*c*) L.-H. Chan, R.-H. Lee, C.-F. Hsieh, H.-C. Yeh and C.-T. Chen, *J. Am. Chem. Soc.*, 2000, **122**, 12385.

18 J. Pommerehne, H. Vestweber, W. Guss, R. F. Mahrt, H. Bässler, M. Porsch and J. Daub, *Adv. Mater.*, 1995, **7**, 551.

19 (*a*) X. H. Zhang, W. Y. Lai, Z. Q. Gao, T. C. Wong, C. S. Lee, H. L. Kwong, S. T. Lee and S. K. Wu, *Chem. Phys. Lett.*, 2000, **320**, 77; (*b*) Y. T. Tao, E. Balasubramaniam, A. Danel and P. Tomasik, *Appl. Phys. Lett.*, 2000, **77**, 933; (*c*) Y. T. Tao, E. Balasubramaniam, A. Danel, B. Jarosz and P. Tomasik, *Appl. Phys. Lett.*, 2000, **77**, 1575; (*d*) Z. Q. Gao, C. S. Lee, I. Bello, S. T. Lee, R.-M. Chen, T.-Y. Luh, J. Shi and C. W. Tang, *Appl. Phys. Lett.*, 1999, **74**, 865; (*e*) X. Jiang, S. Liu, M. S. Liu, H. Ma and A. K.-Y. Jen, *Appl. Phys. Lett.*, 2000, **76**, 2985; (*f*) L. S. Sapochak, A. Padmaperuma, N. Washton, F. Endrino, G. T. Schmett, J. Marshall, D. Fogarty, P. E. Burrows and S. R. Forrest, *J. Am. Chem. Soc.*, 2001, **123**, 6300.

20 G. Jones II, W. R. Jackson, C.-Y. Choi and W. R. Bergmark, *J. Phys. Chem.*, 1985, **89**, 294.

21 C. H. Chen, J. Shi and C. W. Tang, *Coord. Chem. Rev.*, 1998, **171**, 161.

22 (*a*) A. Y. Sonsale, S. Gopinathan and C. Gopinathan, *Indian J. Chem.*, 1976, **14**, 408; (*b*) J. Shi, C. W. Tang and C. H. Chen, *US Patent*, 5645948, 1997.

23 I.-Y. Wu, J. T. Lin, Y.-T. Tao, E. Balasubramaniam, Y.-Z. Su and C.-W. Ko, *Chem. Mater.*, 2001, **13**, 2626.